Technical note: Validation of an ultrahigh dose rate pulsed electron beam monitoring system using a current transformer for FLASH preclinical studies

Patrik Gonçalves Jorge[1] | Veljko Grilj[1] | Jean Bourhis[2] |
Marie-Catherine Vozenin[3] | Jean-François Germond[1] | François Bochud[1] |
Claude Bailat[1] | Raphaël Moeckli[1]

[1] Institute of Radiation Physics, Lausanne University Hospital and University of Lausanne, Lausanne, Switzerland

[2] Radiation-Oncology Department, Lausanne University Hospital and University of Lausanne, Lausanne, Switzerland

[3] Radiation-Oncology Laboratory, Lausanne University Hospital and University of Lausanne, Lausanne, Switzerland

Correspondence
Raphaël Moeckli and Claude Bailat, Institute of Radiation Physics, Lausanne University Hospital and University of Lausanne, Lausanne, Switzerland.
Email: raphael.moeckli@chuv.ch and Claude.bailat@chuv.ch

Abstract

Purpose: The Oriatron eRT6 is a linear accelerator (linac) used in FLASH preclinical studies able to reach dose rates ranging from conventional (CONV) up to ultrahigh (UHDR). This work describes the implementation of commercially available beam current transformers (BCTs) as online monitoring tools compatible with CONV and UHDR irradiations for preclinical FLASH studies.

Methods: Two BCTs were used to measure the output of the Oriatron eRT6 linac. First, the correspondence between the set nominal beam parameters and those measured by the BCTs was checked. Then, we established the relationship between the total exit charge (measured by BCTs) and the absorbed dose to water. The influence of the pulse width (PW) and the pulse repetition frequency (PRF) at UHDR was characterized, as well as the short- and long-term stabilities of the relationship between the exit charge and the dose at CONV and UHDR.

Results: The BCTs were able to determine consistently the number of pulses, PW, and PRF. For fixed PW and pulse height, the exit charge measured from BCTs was correlated with the dose, and linear relationships were found with uncertainties of 0.5 % and 3 % in CONV and UHDR mode, respectively. Short- and long-term stabilities of the dose-to-charge ratio were below 1.6 %.

Conclusions: We implemented commercially available BCTs and demonstrated their ability to act as online beam monitoring systems to support FLASH preclinical studies with CONV and UHDR irradiations. The implemented BCTs support dosimetric measurements, highlight variations among multiple measurements in a row, enable monitoring of the physics parameters used for irradiation, and are an important step for the safety of the clinical translation of FLASH radiation therapy.

KEYWORDS
beam current transformer, charge, dosimetry, FLASH, monitoring, ultrahigh dose rate

1 | INTRODUCTION

Preclinical studies have shown that ultrahigh dose rate (UHDR) irradiations characterized by a doses-per-pulse several orders of magnitude greater than the ones used in clinical practice (typically above 1 Gy per pulse), are able to spare normal tissue while eradicating tumors via the so-called FLASH effect,[1–5] which may lead to

an enhanced therapeutic index in radiotherapy (RT). This effect was observed over several model organisms, such as zebrafish embryos,[2,6] mice,[7–12] cats,[13] mini-pig,[13] and led to the first treatment of a human patient.[14] While FLASH-RT has been mainly characterized using the mean dose rate, this definition has proven to be overly simplistic.[15] The full characterization of FLASH-RT is more complex and involves several interdependent physical parameters of the beam important for the inter-pretation of data. The dose per pulse, number of pulses, time between pulses, pulse width (PW, pulse duration), and instantaneous dose rate (dose rate during pulse duration) are correlated to the biological outcome and might be part of the critical parameters that cause the FLASH effect,[2,6,15–17]

Standard monitoring systems, such as ionization chambers (ICs), typically used in clinical RT linear accel-erators (linacs) cannot be used as monitoring systems in UHDR mode, because of the ion recombination effects due to the ultrahigh dose per pulse.[18–21] Hence, specific dosimetric procedures based on redundant dosimetry have been developed and implemented for preclinical studies to reduce the uncertainties in dose delivery and for regular quality assurance tests.[22–24]

Beam current transformers (BCTs) are widely used in particle accelerator physics mainly for diagnostic measurements of the beam in vacuum, and several studies have shown their high accuracy for charge measurement.[25–30] BCTs are robust and nondestructive devices that enable measurements of charged particle output without affecting the beam. They also provide information on the beam's temporal structure. In the context of the search for the physical beam metric(s) triggering the FLASH effect, this might be highly valu-able information. In addition, the interruption of the beam when the prescription dose is reached during a UHDR irradiation for patient safety remains a challenge from a technological point of view. To address this, BCTs could be incorporated into linac controls to allow them to stop the beam between two consecutive pulses thanks to their fast acquisition and prompt reaction.

A BCT was part of the original Oriatron eRT6 pro-totype linac (PMB-Alcen, France) and used as a diag-nostic system that was developed to count the number of delivered pulses and measure the pulse repetition frequency (PRF) and PW at conventional (CONV) and UHDR.[21] However, this system was placed inside the linac and showed limitations in determining the total exit charge (charge of the electron beam pulses), especially for CONV dose rate irradiations where it was difficult to extract the pulses signal from the noise acquired by the BCT.[21] In addition, the BCTs presented in this study were recently placed at the exit of a modified clinical linac for UHDR irradiations (Mobetron, IntraOp, Sunny-vale, CA, USA) and showed their ability to determine the exit charge with a linear relationship between the delivered dose and the exit charge regardless of the beam parameters (PW and PRF).[31]

TABLE 1 Usual beam parameters for CONV and UHDR modes of the Oriatron eRT6 and related dose per pulse and mean dose rates at a source-to-surface distance (SSD) of 1 m

Mode	GT(V)	PW(μs)	PRF(Hz)	Dose per pulse(Gy)	Mean dose rate(Gy/s)
Range	100–300	0.05–4	5–250		
CONV	100	1.0	10	0.005	0.05
UHDR	300	2.0	100	1	100

Abbreviations: CONV, conventional dose rate; GT, grid tension; PRF, pulse repe-tition frequency; PW, pulse width; UHDR, ultrahigh dose rate.

The initial monitoring system limited our ability to monitor the beam and obtain dosimetric data. Our study aimed to improve the accuracy of the exit charge mea-surement in order to measure in real-time, the delivered dose in predefined radiobiological setups at CONV and UHDR, as presented in Jorge et al.[24] with an accuracy necessary for FLASH preclinical studies, while still being able to extract the essential beam metrics (number of pulses, PRF, and PW). We implemented a commercially available BCT as a beam monitoring instrument at the exit of the Oriatron eRT6 linac , first testing the BCT's ability to accurately reconstruct the aforementioned parameters of the delivered beam. In our search to use the BCT as a beam monitor system, we investigated the relationship between the exit charge measured by the BCT and the absorbed dose to water in reference setups, and the influence of beam parameters on that relationship, as well as the short- and long-term stability of the dose-to-charge ratio.

2 | MATERIALS AND METHODS

2.1 | Linac and beam characteristics

The Oriatron eRT6 delivers a 5.4 MeV pulsed electron beam, with doses per pulse ranging from conventional ($\sim$mGy) to ultrahigh (>10 Gy) and total irradiation times ranging from minutes to microseconds. The functioning of the linac has been described elsewhere.[21,24] Briefly, the Oriatron eRT6 is able to increase the dose per pulse mainly by varying the grid tension (GT), which controls the number of electrons extracted from the cathode. Additionally, the number of pulses (N_p), the PW, and the PRF can all be set independently.

We operated the accelerator in CONV mode mimick-ing the configuration of a clinical beam and UHDR mode. Table 1 presents the usual beam parameters used in CONV and UHDR modes.

2.2 | Dosimetric instruments and setup

The absorbed dose to water was determined either with the Advanced Markus IC (PTW-Freiburg,
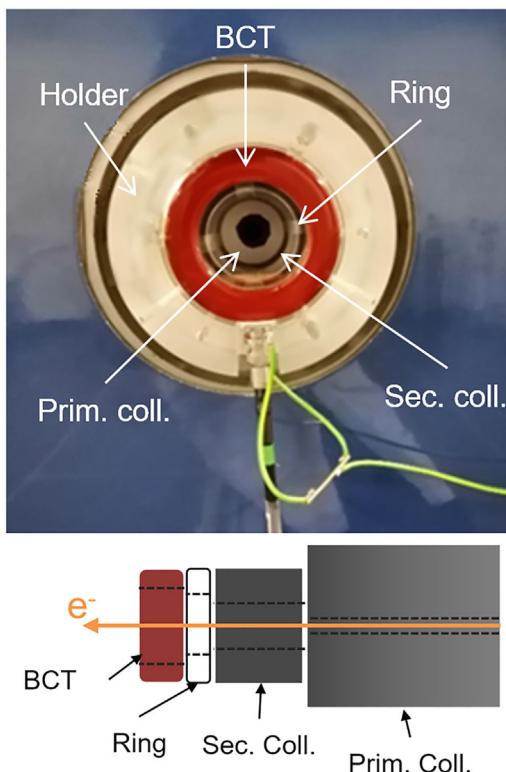
FIGURE 1 Picture of the holder at the exit of the linac (top) and scheme of the complete setup showing the beam current transformer (BCT), a PMMA ring, and both secondary and primary carbon collimators (bottom). The physical apertures of these devices were 55, 50, 40, and 12.4 mm, respectively. The inner diameters of the manufactured elements were chosen based on lateral dose profiles acquired at the same position

Germany) coupled with a PTW UNIDOS electrometer or by GafChromic EBT3 films (Ashland Specialty Ingredients G.P., Bridgewater, NJ, USA). The IC-associated overall uncertainties are 1.6 % in CONV mode and 2.8 % in UHDR mode (chamber-specific model).[22] The IC chamber was used for absolute dosimetry in CONV mode (Section 2.3.3), as well as for the stability of the dose-to-charge ratio in both modes (Section 2.3.2). The EBT3 films were used for absolute dosimetry at UHDR with an uncertainty of 2 % (Section 2.3.3). Their use is reported in detail elsewhere.[21,23]

Absorbed dose measurements were performed at 15-mm depth in a 15-cm thick solid water phantom made of 30 × 30 cm^2 RW3 slabs (PTW-Freiburg, Germany) positioned at a source-to-surface distance of 0.8 m. Film measurements showed that the beam produced a circular field of approximately 16-cm diameter (FWHM) of Gaussian shape at 15-mm depth.

2.3 | Beam monitoring system

A custom-made PMMA holder was designed to install the BCT at the exit of the linac (Figure 1). To minimize the amount of dose received by the BCT and extend

its lifetime, a secondary carbon collimator was placed inside the holder between the linac primary collimator and the BCT to act as a shielding. A PMMA ring was added between the secondary collimator and the BCT to reduce the electrical noise originating from the reflected radio frequency in the accelerator cavity and act as an insulator. The impact of the holder and its components on the primary electron beam was evaluated through dose profile measurements and was found to be negligible within the film uncertainty.

The newly mounted BCT is an ACCT (version with bandwidth extension to 3 MHz) from Bergoz Instrumentation[32] that consisted of a toroid sensor, an external electronic system, and a power supply. Two BCTs were placed at the exit of the linac and equipped with their dedicated acquisition and signal processing electronics defining the operating full scales: 10 mA (peak current) for irradiations with a low GT (100 V) in CONV mode and 300 mA (peak current) when using the highest GT (300 V) in UHDR mode. Each BCTs was calibrated with its own readout electronics so that we had to keep both parts together at any time. Both BCTs had an upper bandwidth limit of 3 MHz acting as a low-pass filter,[32] a rise time of about 110 ns (10 %–90 %), and a signal drop of about 0.4 % per millisecond (data provided by the firm).

Output signals from the BCTs were acquired by a NI PXIe-5114 oscilloscope module seated in a PXIe-1071 chassis (National Instruments, USA). One channel was allocated to each BCT. Each channel had a sampling frequency of 125 × 10^6 samples per second with 8-bit resolution and 125 MHz bandwidth. Because of the small bandwidth of the BCTs, the sample rate exceeded twice the instrument bandwidth and aliasing was avoided. The sampling frequency and the BCT's rise times did not allow us to distinguish the magnetron frequency pulse microstructure (3 GHz).

Signals from the BCTs were displayed and recorded with a homemade LabVIEW 2014 code (National Instruments, USA). The oscilloscope trigger level was specified by a voltage threshold at 0.04 V for both BCTs, and the rising edge of the pulses was positioned at 5.5 μs with respect to the total 10 μs record for each waveform.

After the acquisition, data in both modes were processed to quantify the total exit charge as follows: first, recorded waveforms were filtered using a low-pass filter with a cutoff frequency of 20 MHz to suppress the high-frequency noise from the unshielded linac; second, the baseline offset was determined for each waveform by averaging the signal over the first 5 μs and then subtracted; third, the BCT voltage value from a given measurement was converted into a current based on the calibration coefficients provided by the manufacturer[32]; finally, the integration of the current over time resulted in the value for the exit charge of electrons. Because of the very low droop of the ACCT, the length of integration window had a negligible influence on the integration value.

2.3.1 | Measurement of beam parameters

For a series of irradiations, the main beam parameters (N_p, PRF, and PW) were measured by the BCT system and compared to the ones specified by the user within the linac operating software: N_p between 2 and 100, PRF between 5 and 250 Hz, PW between 1 and 4 μs, and GT values of 100 V (CONV) and 300 V (UHDR). The PW was defined as the time between the 10 % reference level instants.

2.3.2 | Stability of the dose-to-charge ratio

The absorbed dose to water was simultaneously measured (by the IC) as a function of the exit charge (from the BCTs), and the dose-to-charge ratio was computed to account for variations in daily measurements due to the change in the machine output.

The dose-to-charge ratio was investigated in delivering 1030 pulses (CONV) and 15 pulses (UHDR) and always the same PWs (Table 1). The procedure was repeated every day of machine use (40 days), and each measurement was performed 10 times a day. Short-term stability was evaluated by computing the standard deviation (SD) of the dose-to-charge ratio over the daily measurements. Long-term stability was assessed by analyzing the variation in the mean daily values of the dose-to-charge ratio over the whole period as well as the SD.

2.3.3 | Charge–dose relationship

In CONV mode, the dose was measured by the IC and was varied by changing only N_p from 100 to 2100 in analogy with CONV-RT, resulting in absorbed doses to water varying between 0.5 and 11 Gy. The other beam parameters were kept as described in Table 1. Simultaneously, the BCT was monitoring the exit charge.

In UHDR mode, dose measurements were performed with GafChromic films together with charge measurements from the BCT. Films were preferred to the ionization chamber in that case because GafChromic films are independent of the pulse dose rate and, unlike ICs, do not need corrections for recombination.[22] To assess the influence of f on the charge–dose relationship, a series of measurements were performed with PRFs of 10, 100, and 250 Hz according to the beam parameters in Table 2. Each series of measurements resulted in a charge–dose relationship where N_p was varied with a fixed PRF. Then, to investigate the dependency of PW on the charge–dose relationship, PWs equal to 0.5, 2, and 4 μs were chosen with beam parameters from Table 2. Each series of measurements resulted in a charge–dose relationship where N_p was varied with a fixed PW. In both cases, a set of eight values of N_p was

adapted to cover a dose range between 2 and 18 Gy approximately (Table 2).

3 | RESULTS

3.1 | Measurement of beam parameters

All beam parameters characterizing the temporal structure of the beam acquired with the software coupled with the BCT were all in accordance with the parameters set on the Oriatron eRT6 (N_p, PRF, and PW) for all parameter combinations tested. The software coupled with the BCT was consistently able to determine the number of delivered pulses. Regarding the PRF, the computed PRF from the rising edge of the pulse signal allowed the software to determine the PRF with high accuracy (deviations <0.01 %). Finally, the comparison between the PWs set on the Oriatron eRT6 and the ones measured by the BCT agreed with a maximum deviation of about 5 %. An illustration of the data recorded by the BCTs is shown in Figure 2 where the normalized signals of pulses of different PWs (UHDR) are displayed together with a CONV pulse.

The integrated charge of each pulse, the mean value of all pulses, SD, and the sum of integrated charges of all pulses were calculated as well (corresponding to the mean value multiplied by the number of pulses). The dose per pulse, the instantaneous dose rate within the pulse, and the beam-on time were extracted from the recorded data. Typical SDs for the integrated charge were 3 % and 1 % in CONV and UHDR mode, respectively. The low-current BCT (10 mA) allowed measurements of pulses down to 0.1 mA with a good signal-to-noise ratio, while the high-current BCT (300 mA) is able to perform measurements up to 300 mA, resulting in a total dynamic range of 3000.

For comparison purposes with the initial monitor system, Figure 3 shows the raw signal of a UHDR pulse measured by both systems.

TABLE 2 UHDR beam parameters used to investigate the PRF and PW dependency of the charge–dose relationship

Parameter investigated	GT(V)	PW(μs)	PRF(Hz)	N_p
F	300	2	10	1–8
			100	
			250	
W	300	0.5	100	3–35
		2		1–12
		4		1–8

Note: Regarding the number of pulses, the minimum and maximum values are indicated, but only a set of eight values were selected in this range.

Abbreviations: GT, grid tension; N_p, number of pulses; PRF, pulse repetition frequency; PW, pulse width; UHDR, ultrahigh dose rate.

FIGURE 2 Normalized raw signal of a conventional (CONV) pulse (orange circles) and ultrahigh dose rate (UHDR) pulses (1.4, 2.4, and 3.5 μs pulse widths [PWs]) measured by the beam current transformers (BCTs) presented in this paper
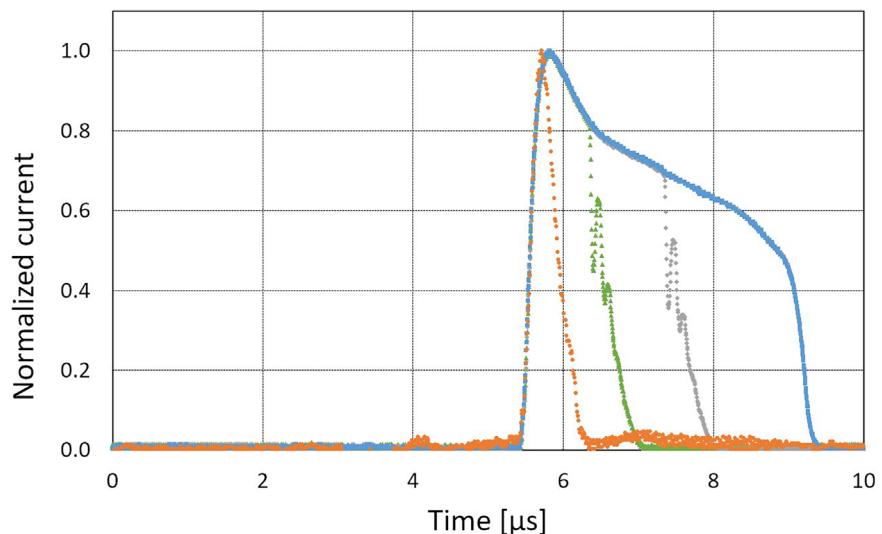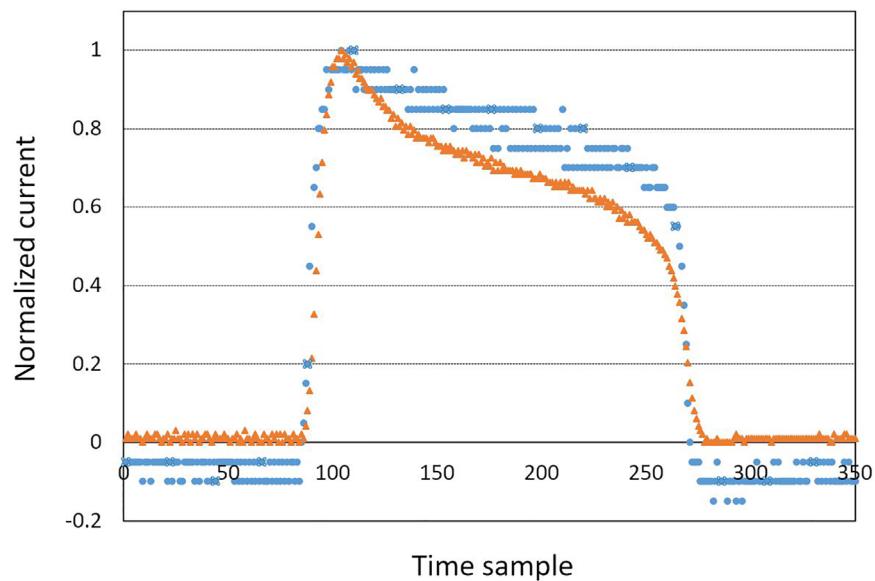

FIGURE 3 Comparison of the normalized raw signal from the initial monitor system (blue circles) and the newly mounted beam current transformer (BCT) (orange triangles) for same ultrahigh dose rate (UHDR) pulse

3.2 | Stability of the dose-to-charge ratio

Short-term stability of the dose-to-charge ratio in terms of SD was below 0.5 % (CONV) and 1.4 % (UHDR).

For the long-term stability, SDs were 0.9 % (CONV) and 1.5 % (UHDR). Maximum deviations with respect to the mean ratio remained below 1.6 % and 2.3 % in CONV and UHDR modes, respectively.

3.3 | Charge–dose relationship

Figure 4 shows a linear relationship between the dose measured by the IC and the exit charge in CONV mode. Relative deviations of the data points with respect to the fitting curve remained below 0.6 %.

In UHDR mode, a linear relationship was found between the dose measured by the EBT3 films and the

exit charge for PW of 0.5, 2, and 4 μs. For all investigated PWs, the distribution of measurement points was well represented by a linear relation, and the slope of the fitting curve decreased with PW. For each PW, the relative deviations between the data points and the respective fitting curve remained under 3 % (Figure 4).

The impact of PRF on the charge–dose relationship was found to be negligible as shown in Figure 5 (within the uncertainty of the films).

4 | DISCUSSION

We implemented BCTs on the Oriatron eRT6 linac and studied their capability to monitor a pulsed electron beam delivered in a reproducible way in both CONV and UHDR modes as an improvement with respect to the initial system presented in Jaccard et al.[21] The processing of the data from the BCTs was much simpler because of
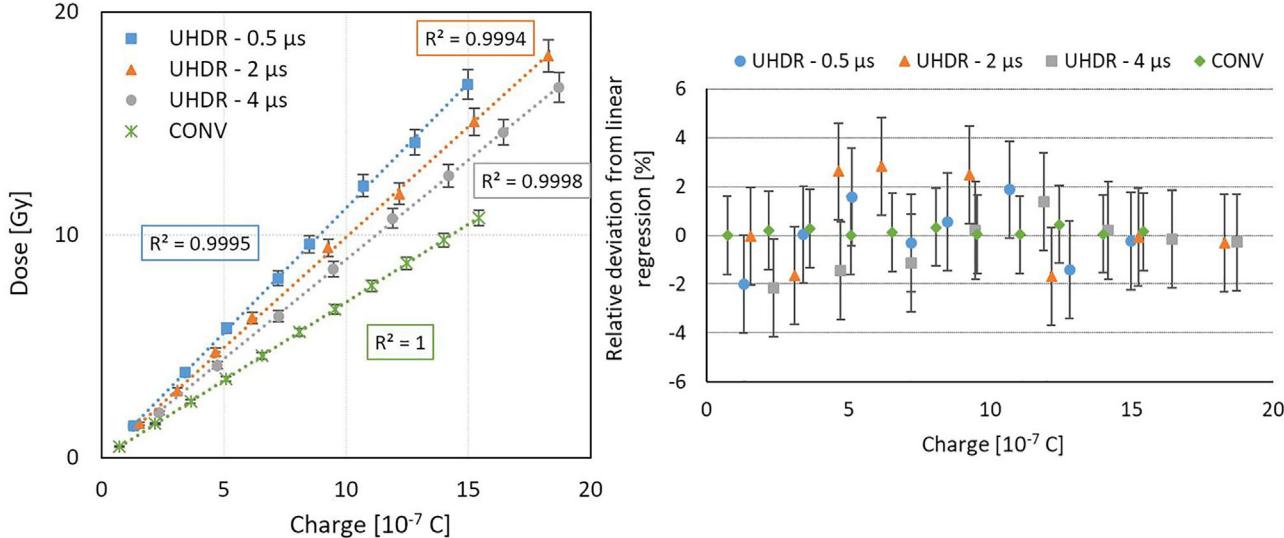
FIGURE 4 Absorbed dose to water as a function of the exit charge measured by the beam current transformers (BCTs) in conventional (CONV) (green diamond) and ultrahigh dose rate (UHDR) modes for pulse width (PW) = 0.5 μs (blue squares), 2 μs (orange triangles), and 4 μs (gray disks) (left) (see Table 2). Relative deviations from the linear regression are also shown (right). Uncertainty bars correspond to the expanded uncertainty ($k = 2$). The uncertainty related to the charge measurement (horizontal axis) is hidden by the measurement point because of its small value. The change of slope in UHDR mode between the different PWs is due to variations in the percentage depth dose curves between each PW.
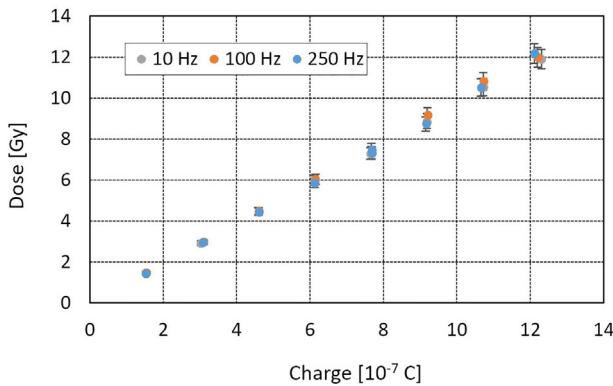

FIGURE 5 Absorbed dose to water as a function of the exit charge measured by the beam current transformers (BCTs) in ultrahigh dose rate (UHDR) mode for pulse repetition frequency (PRF) = 10, 100, and 250 Hz (see Table 2)

their dedicated acquisition and signal processing electronics compared to the initial system. The measuring range was adapted to the signals with the new system allowing a better resolution of the pulses as shown in Figure 3. Finally, these BCTs were also able to provide all the physical beam parameters as the previous monitoring system without showing any measurable effect on the beam.

This independent monitoring system accurately reconstructed the main beam parameters (N_p, PRF, and PW) in both modes as the previous system, which makes it a suitable diagnostic tool for the linac control that helps to point out issues occurring during delivery. Furthermore, N_p, PRF, and PW were determined for

any irradiation. This last feature can prove particularly useful for investigating the role of the different beam metric(s) triggering the FLASH effect and establish a pattern between the beam parameters. A dedicated monitoring device measuring the physical beam parameters is essential for all FLASH studies in order to perform correlations between the biological endpoint and the beam parameters used. This is why the main beam parameters need to be properly documented to evaluate if the delivery conditions are optimal and ultimately define the parameter(s) that is(are) relevant to trigger the FLASH effect.

In addition to the previous beam monitoring system described in Jaccard et al.,[21] the high-precision BCT was able to measure low beam currents such as those used for irradiations in CONV mode and allowed measurements with a much less noisy signal in both CONV and UHDR modes (Figure 2), and led to the computation of a linear relationship between the delivered dose and the exit charge with relative deviations smaller than 1 % (Figure 4).

The stability of the dose-to-charge ratio was found better than 1.5 % for CONV, but UHDR stability was systematically larger, probably because of the combined uncertainties from the eRT6 beam characteristic variations and the related detectors' response. For example, the spatial energy distribution of the beam might change and affect the IC reading, but not the BCT. These effects are entangled and hard to deconvolute in a system without solid references. Still, in UHDR mode, the stability of the dose-to-charge ratio (short- and long-term) was better than the stability of the linac itself, and was of the

same order of magnitude or better than the values measured on a medical pulsed electron linac modified for UHDR RT.[21,31]

Our study found the charge–dose relationship in UHDR mode to be linear, and no dependence on PRF to within a certain tolerance defined by the combined uncertainty of our measurements was observed, which enabled us to change the time interval between pulses and thus modify the irradiation time and mean dose rate while keeping the same dose-to-exit charge ratio.

At UHDR for a given exit charge, the dose deposited in the target at the beam center at a fixed depth decreased when PW was increased (Figure 4). This can be explained by a reduction in the beam penetration in matter, thereby in the energy, when increasing the charge per pulse. This phenomenon was already observed during the linac commissioning and was attributed to the fixed maximum power of the magnetron, which limits the acceleration process.[21] This PW dependency was not investigated with the previous monitoring system. However, no PW dependency was observed on another machine with the same BCTs where it was shown that the beam energy did not change with PRF or PW.[31,33] This nonlinear relationship does not discredit the use of BCTs for the Oriatron eRT6 but means that we have to calibrate each setup for each PW planned for the biological experiment.

Measurements of the BCT signal enabled us to compute the delivered dose based on the exit charge in a similar way to the transmission chambers and monitor units (MU) defining the absorbed dose in clinical practice in specific reference conditions in both CONV and UHDR modes. These results can be extended to other setups than the one presented using our methodology, as the BCTs can monitor the linac output while the delivered dose depends strongly upon the geometrical conditions. The development of a control system bridging the gap between the machine and the monitoring presented in this paper would be a first step to ensure pulse counting for a routine clinical use.

5 | CONCLUSIONS

We improved the beam monitoring system on the eRT6 thanks to commercially available BCTs that were able to monitor a pulsed electron beam delivered in CONV and UHDR modes that can be used in preclinical and further clinical studies for FLASH. The absorbed dose can be derived in real time from the previously calibrated BCT signal during irradiations without affecting the beam and without having to apply any corrections that may arise due to signal saturation in UHDR mode. The implementation of the BCTs simplifies dosimetric procedures, increases repeatability of the experimental conditions, and enables the delivered dose to be estimated with an accuracy required for preclinical studies

in both CONV and UHDR modes. Moreover, this system might be implemented in future linacs using UHDR for clinical patient irradiations, and could be the base for real-time controlling of the UHDR output.

CONFLICT OF INTEREST
The authors have no relevant conflicts of interest to disclose.

DATA AVAILABILITY STATEMENT
The data that support the findings of this study are available from the corresponding author upon reasonable request.

REFERENCES
1. de Kruijff RM. FLASH radiotherapy: ultra-high dose rates to spare healthy tissue. *Int J Radiat Biol*. 2020;96(4):419-423. https://doi.org/10.1080/09553002.2020.1704912
2. Vozenin MC, Hendry JH, Limoli CL. Biological benefits of ultrahigh dose rate FLASH radiotherapy: sleeping beauty awoken. *Clin Oncol (R Coll Radiol)*. 2019;31(7):407-415.
3. Hendry J. Taking care with FLASH radiation therapy. *Int J Radiat Oncol Biol Phys*. 2020;107(2):239-242. https://doi.org/10.1016/j.ijrobp.2020.01.029
4. Durante M, Brauer-Krisch E, Hill M. Faster and safer? FLASH ultra-high dose rate in radiotherapy. *Br J Radiol*. 2018;91(1082):20170628.
5. Wilson JD, Hammond EM, Higgins GS, Petersson K. Ultra-high dose rate (FLASH) radiotherapy: silver bullet or fool's gold? *Front Oncol*. 2019;9:1563.
6. Bourhis J, Montay-Gruel P, Goncalves Jorge P, et al. Clinical translation of FLASH radiotherapy: why and how? *Radiother Oncol*. 2019;139:11-17.
7. Favaudon V, Caplier L, Monceau V, et al. Ultrahigh dose rate FLASH irradiation increases the differential response between normal and tumor tissue in mice. *Sci Transl Med*. 2014;6(245):245ra293.
8. Montay-Gruel P, Acharya MM, Petersson K, et al. Long-term neurocognitive benefits of FLASH radiotherapy driven by reduced reactive oxygen species. *Proc Natl Acad Sci U S A*. 2019;116(22):10943-10951.
9. Montay-Gruel P, Petersson K, Jaccard M, et al. Irradiation in a flash: unique sparing of memory in mice after whole brain irradiation with dose rates above 100Gy/s. *Radiother Oncol*. 2017;124(3):365-369.
10. Montay-Gruel P, Bouchet A, Jaccard M, et al. X-rays can trigger the FLASH effect: ultra-high dose rate synchrotron light source prevents normal brain injury after whole brain irradiation in mice. *Radiother Oncol*. 2018;129(3):582-588.

11. Smyth LML, Donoghue JF, Ventura JA, et al. Comparative toxicity of synchrotron and conventional radiation therapy based on total and partial body irradiation in a murine model. *Sci Rep*. 2018;8:12044.

12. Diffenderfer ES, Verginadis II, Kim MM, et al. Design, implementation, and in vivo validation of a novel proton FLASH radiation therapy system. *Int J Radiat Oncol Biol Phys*. 2020;106(2):440-448.

13. Vozenin MC, De Fornel P, Petersson K, et al. The advantage of FLASH radiotherapy confirmed in mini-pig and cat-cancer patients. *Clin Cancer Res*. 2019;25(1):35-42.

14. Bourhis J, Sozzi WJ, Jorge PG, et al. Treatment of a first patient with FLASH-radiotherapy. *Radiother Oncol*. 2019;139:18-22.

15. Vozenin MC, Montay-Gruel P, Limoli C, Germond JF. All irradiations that are ultra-high dose rate may not be FLASH: the critical importance of beam parameter characterization and in vivo validation of the FLASH effect. *Radiat Res*. 2020;194(6):571-572.

16. Griffin RJ, Ahmed MM, Amendola B, et al. Understanding high-dose, ultra-high dose rate and, spatially fractionated radiotherapy. *Int J Radiat Oncol Biol Phys*. 2020;107(4):766-778. https://doi.org/10.1016/j.ijrobp.2020.03.028

17. Moeckli R, Germond JF, Bailat C, Bochud F, Vozenin MC, Bourhis J. Bringing FLASH to the clinic. *Int J Radiat Oncol*. 2020;107(5):1012-1013.

18. Mujsolino SV. Absorbed dose determination in external beam radiotherapy: an international code of practice for dosimetry based on standards of absorbed dose to water; technical reports series no. 398. *Health Phys*. 2001;81(5):592-593.

19. Almond PR, Biggs PJ, Coursey BM, et al. AAPM's TG-51 protocol for clinical reference dosimetry of high-energy photon and electron beams. *Med Phys*. 1999;26(9):1847-1870.

20. Karsch L, Beyreuther E, Burris-Mog T, et al. Dose rate dependence for different dosimeters and detectors: TLD, OSL, EBT films, and diamond detectors. *Med Phys*. 2012;39(5):2447-2455.

21. Jaccard M, Duran MT, Petersson K, et al. High dose-per-pulse electron beam dosimetry: commissioning of the Oriatron eRT6 prototype linear accelerator for preclinical use. *Med Phys*. 2018;45(2):863-874.

22. Petersson K, Jaccard M, Germond JF, et al. High dose-per-pulse electron beam dosimetry - a model to correct for the ion recombination in the advanced Markus ionization chamber. *Med Phys*. 2017;44(3):1157-1167.

23. Jaccard M, Petersson K, Buchillier T, et al. High dose-per-pulse electron beam dosimetry: usability and dose rate independence of EBT3 gafchromic films. *Med Phys*. 2017;44(2):725-735.

24. Jorge PG, Jaccard M, Petersson K, et al. Dosimetric and preparation procedures for irradiating biological models with pulsed electron beam at ultra-high dose rate. *Radiother Oncol*. 2019;139:34-39.

25. Schutte W, Unser KB. Beam current and beam lifetime measurements at the HERA proton storage-ring. *AIP Conf Proc*. 1993;281:225-233. https://doi.org/10.1063/1.44341

26. Unser K. A toroidal DC beam current transformer with high-resolution. *IEEE Trans Nucl Sci*. 1981;28(3):2344-2346.

27. Unser KB. The parametric current transformer, a beam current monitor developed for LEP. *AIP Conf Proc*. 1992;252:266-275.

28. Unser KB. Toroidal AC and DC current transformers for beam intensity measurements. *Atomkernenerg Kernt*. 1985;47(1):48-52.

29. Bergoz J. Current monitors for particle beams. *Nucl Phys A*. 1991;525:C595-C600.

30. Torp B, Abrahamsen P, Eriksen S, Hoeg PL, Nielsen BR, Bergoz J. Non-intercepting continuous beam current measurement for a high-current ion implanter. *Surf Coat Technol*. 1994;66(1-3):361-363.

31. Oesterle R, Goncalves Jorge P, Grilj V, et al. Implementation and validation of a beam-current transformer on a medical pulsed electron beam LINAC for FLASH-RT beam monitoring. *J Appl Clin Med Phys*. 2021;22(11):165-171. https://doi.org/10.1002/acm2.13433

32. Bergoz Instrumentation, ACCT. Bergoz Instrumentation. Accessed February 24, 2020. https://www.bergoz.com/en/acct

33. Moeckli R, Goncalves Jorge P, Grilj V, et al. Commissioning of an ultra-high dose rate pulsed electron beam medical LINAC for FLASH RT pre-clinical animal experiments and future clinical human protocols. *Med Phys*. 2021;48(6):3134-3142. https://doi.org/10.1002/mp.14885